Stenosis assessment via volumetric flow rate calculation

Andrey I. Svitenkov[1][0000-0002-2676-0820], Pavel S. Zun[1,2][0000-0001-6176-1143] and
Oleg A. Shramko[1][0000-0002-2793-1951]

[1] ITMO University, Saint Petersburg, 197101, Russia
[2] University of Amsterdam, Amsterdam, 1098 XH, The Netherlands
aisvitenkov@itmo.ru
oashramko@itmo.ru
p.zun@uva.nl

Abstract. Coronary artery stenosis is a condition that restricts blood flow to the myocardium, potentially leading to ischemia and acute coronary events. To decide whether an intervention is needed, different criteria can be used, e.g. calculation of fractional flow reserve (FFR). FFR can also be computed based on computer simulations of blood flow (virtual FFR, vFFR). Here we propose an alternative, more direct, metric for assessing the hemodynamic value of stenosis from computational models, the computed volumetric flow drop (VFD). VFD and vFFR are computed for several stenosis locations using a 1D model of the left coronary tree, and also an analytical model is presented to show why FFR value may differ from the true flow reduction. The results show that FFR = 0.8, which is often used as a criterion for stenting, may correspond to a reduction in volumetric flow from less than 10% to almost 30% depending on the stenosis location. The implications are that FFR-based assessment may overestimate the hemodynamic value of stenosis, and it's preferable to use a more direct metric for simulation-based estimation of stenosis value.

Keywords: fractional flow reserve, stenosis, blood flow model, lumped model, coronary arteries

1   Introduction

Arterial stenosis is a pathological condition of an artery, characterized by a narrowing of its lumen. Stenting is often used to eliminate this defect. This invasive procedure consists in expanding the narrowed vessel and implanting a special mesh (a stent) into the wall of the vessel, which prevents the artery from re-narrowing.

In clinical practice it is important to assess the physiological importance of a particular arterial stenosis. This way, the treatment of coronary artery disease can be planned and improved. Currently, it is assessed by using a parameter called *fractional flow reserve* (FFR). According to the work [1], FFR is defined as the maximal blood flow in the presence of a stenosis in the artery, divided by the theoretical normal maximal flow in the same vessel. In practice FFR is calculated as the ratio of two pressure values: P_d, which is measured distally from the stenosis and P_p, measured proximally from it [2]. The question arises how to estimate the proximal and the distal pressures.

In clinical practice the mean pressure in the aorta (P_a) is usually substituted for P_p [3] and both pressures are measured during maximum hyperemia, which is an approximation [4, 5, 6].

In addition to invasive measurement, FFR can also be calculated from a numerical simulation of flow through the stenosis. By simulating the flow, the pressure across the stenosis (ΔP_{st}) can be obtained. If the proximal pressure is known, ΔP_{st} can be used to calculate the virtual FFR, also called vFFR.

The FFR is first mentioned in the article [4], where this concept is introduced to assess the severity of stenoses. In that work, a model of coronary circulation is considered, in which the stenosis is located in an artery. The artery is connected to the aorta on one side of the stenosis; on the other side it is connected to collateral vessels and the myocardial vascular bed. Starting with that work, aortic pressure has been used in the FFR calculations, and P_a is also used later in other works even with other topologies, with rare exceptions [2], although it would be more correct to use the proximal pressure.

There are many works in which vFFR is found through the pressure ratio. These works apply computational fluid dynamics to simulate hemodynamics and ultimately to obtain the pressures required to calculate vFFR. For this, first, computer anatomical models are created based on angiograms. Moreover, both non-invasive MRI data and invasive angiography can be used. The latter case seems less preferable, because one of the purposes of using vFFR is to avoid surgical interventions. In [7], a summary of vFFR models is given, comparing their accuracy against an invasively measured FFR value. Another study [8] presents four different computational methodologies for finding vFFR. In all cases, the required value is obtained as the ratio of P_d to P_a. Depending on the methodology P_a is either the mean aortic pressure, or a mean pressure at a point proximal to the stenosis. One of the methodologies states that P_a is found as the spatial average at the inlet region of approximately 2 mm length, and the region is defined manually.

When assessing the severity of stenosis, the main physiological quantity of interest (QOI) is the change in blood flow through the artery. However, a pressure-based assessment is used in clinical practice, because it is independent from the baseline flow, relatively simple and cost effective [9]. Following this method, vFFR is also calculated from pressures.

The idea of using volumetric flow rates ratios instead of pressure ratios in numerical calculations to assess the importance of stenosis is not new. In [10], a method for calculating the vFFR by constructing a lumped parameter model from angiograms was proposed. FFR$_{angio}$ is found as the ratio of the maximal flow rate in the stenosed artery and the maximal flow rate in the absence of the stenosis. The research results have shown that FFR$_{angio}$ has a high sensitivity, specificity, and accuracy when compared to clinical FFR (diagnostic accuracy is 92.2%).

Here we propose an alternative method, using the volumetric flow rate values in the artery with a stenosis (Q_s) and the flow rate in the same artery, but without a stenosis (Q_0). These values can be found from numerical modeling of blood circulation in the coronary vessels. In our study, a 1D model is built with boundary conditions specified by a 0D model. The proposed method is compared to the vFFR results.

Given the primary importance of the volumetric flow rate values and the fact that in any case, the calculation of vFFR requires modeling using the coronary artery system, the estimation of the change in flux seems preferable.

2 Illustration of the idea

We have noted before that the decrease in the volumetric flow rate due to a stenosis has a direct physiological impact. Here we will present an analytical lumped model of coronary arteries to illustrate the relation between FFR and the volumetric flow rate in the artery with and without stenosis: Q_s and Q_0.

For this purpose, we consider a simplified steady state model of coronary arteries (CA). Represented by hydrodynamic resistance elements, the arteries form the hierarchical structure shown in Fig. 1A. The resistance R_σ is the resistance of the considered stenosis, R_i are for resistive arterial segments between bifurcations and R_{Ti} are for resistances of peripheral vessels.

We are looking for an expression of the pressure proximal and distal to the stenosis and of the flow through the stenosis as a function of all resistances in the model. Unfortunately, even for this simplified representation these expressions turn out to be very complex and do not have much illustrative use. For further simplification, we consider that the resistance of major arteries is much smaller than the resistance of peripheral arteries, arterioles and capillaries. Then the CA structure can be represented as a set of parallel branches (Fig. 1B) and, finally, just by two branches as in the Fig. 1C. The resistance R_S here represents all parallel branches of CA, it decreases with the number of branches N proportionally to $1/N$. The same is correct for R_{T0}: representing the resistance of all distal parts of CA, it is smaller for more proximal positions of the stenosis (because the number of capillaries downstream is larger).

(A)	(B)	(C)
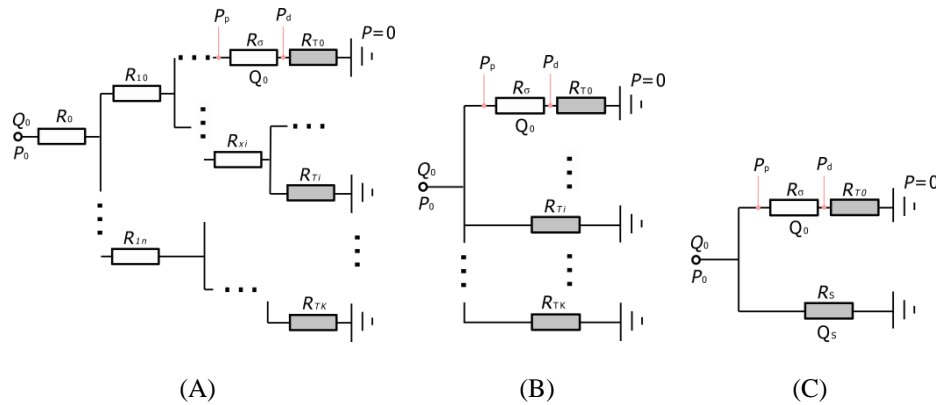
Fig. 1. Lumped steady-state model of CA. (A) The most detailed representation; (B) resistances of arterial segments are presumed negligible comparing with resistance of peripheral arteries; (C) the most simple representation.

For the model from Fig. 1C the values of P_d and P_p can be easy calculated, as well as the FFR value:

$$FFR = \frac{P_d}{P_p} = \frac{R_{T0}}{R_\sigma + R_{T0}} \ . \tag{1}$$

To estimate the flux through the stenosis we need to consider how the inlet boundary condition is set: that is, either by a prescribed pressure or by flux. In case of a prescribed pressure, the relation between the flux through the stenosis Q_σ and the flux for the same location without a stenosis $Q_{\sigma 0}$ gives the same expression as (1). Thus, FFR can be considered an approximation of the relation $Q_\sigma/Q_{\sigma 0}$ for fluxes, which has a direct physiological meaning. We will call this relation Volumetric Flux Drop (VFD) in the following. In practical terms it can be considered as a measure of *how much the flux through the stenosis decreases after stenting.*

Similar conclusions were stated by *Pijls et al.* with an introduction of FFR [4]. We, however, would also like to consider the case where the inlet flux is prescribed since we believe that it represents the real situation better. Cardiac compensation increases the arterial pressure in response to the increasing resistance of coronary arteries to provide the normal blood supply to the heart muscle [11]. We can emphasize this argument by considering the structure (C) as a part of structure (A) (see Fig. 1). Then the inlet point corresponds not to the aortic sinus but to some bifurcation of the CA. The inlet pressure then will change in response to a changing stenosis resistance as well as the inlet flux. Both choices are reasonable, but the choice of a constant flux is better since it takes the compensatory mechanisms into the account.

For the case of a prescribed inlet flux, the expression for the VFD value is different:

$$VFD = \frac{Q_\sigma}{Q_{\sigma 0}} = \frac{R_{T0} + R_S}{R_\sigma + R_{T0} + R_S} = 1 - \frac{R_\sigma}{R_\sigma + R_{T0} + R_S} \ . \tag{2}$$

If the resistance R_S of all side branches is negligible compared to R_{T0}, then VFD tends to FFR. However, considering the last expression, we may see that the FFR value underestimates the VFD.

The presented illustration shows that even for a very simplified model of CA we clearly see the difference between VFD and FFR. We should expect an even larger discrepancy for the real situation due to a more complex structure of CA and a pulsatile blood flow.

3   1D numerical model

In this study, numerical modeling of hemodynamics in the system of coronary arteries was carried out. For this, the following 1D model was used.

The model formulation based on the equations relating the average velocity U and the area of the vessel lumen A was used:

$$\begin{cases} \frac{\partial A}{\partial t} + \frac{\partial AU}{\partial x} = 0 \\ \frac{\partial U}{\partial t} + U\frac{\partial U}{\partial x} + \frac{1}{\rho}\frac{\partial P}{\partial x} = \frac{8\mu\pi U}{\rho} \end{cases}, \tag{3}$$

where t is time, x is the longitudinal coordinate relative to the artery, ρ is the blood density, P is the pressure in the discretization point, μ is the dynamic blood viscosity.

The model takes into the account the elastic properties of the arteries, with Young's modulus $E = 225\ kPa$. The thickness of arteries' walls h depends on the reference radius of a vessel [12] as $h = r_0(a \cdot exp(br_0) + c \cdot exp(dr_0))$, where $a = 0.2802$, $b = -5.053\ cm^{-1}$, $c = 0.1324$, $d = -0.1114\ cm^{-1}$, r_0 is an arterial radius at diastolic pressure.

All other parameters considered for the blood flow model are presented in the Table 1.

Table 1. General parameters of blood flow model for all simulations.

Property	Value
Blood density, ρ, kg·m^{-3}	1040
Blood viscosity, μ, mPa·s	3.5
Velocity profile order, ζ	9
Young's modulus, E, kPa	225.0
Space discretization step, mm	2.5
Timestep, ms	0.05

The outlet boundary conditions replacing the downstream vasculature were represented by RCR Windkessel elements [13]. A known flow rate with a ninth order velocity profile defines an inlet BC.

We consider a geometrical model of CA provided by Zygote (Zygote Media Group, Inc.) and constructed as a compilation of multiple CT models of coronary arteries for most typical anatomies (Fig. 2A).

(A)   (B)
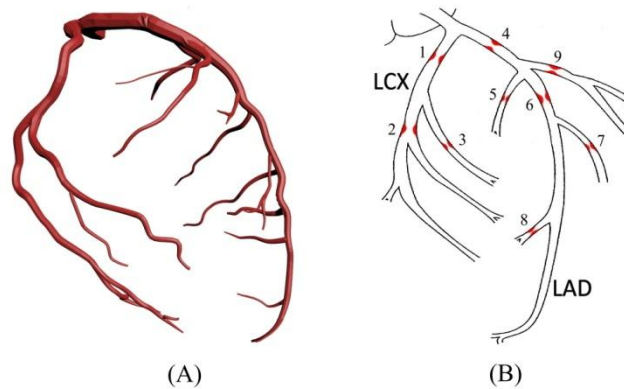
Fig. 2. Coronary arteries. (A) General appearance of the considered model of the LCA tree; (B) stenosis locations during the simulations (marked in red).

Given the high variability of CA we should note insufficiency of such approach for reaching definitive conclusions. Population studies that consider a set of patient-specific geometries would be more preferable, but require the data we do not have.

Nevertheless, considering a single and typical arterial structure provides an assessment of relation between vFFR and VFD for various positions of stenosis.

The 3D structure of CA has been translated to a 1D geometry by centerline detection followed by prescribing arterial radius in each discretization point along the centerline in accordance with the area of arterial lumen in the corresponding section.

The coronary arteries collectively form two networks, which originate from the right coronary artery (RCA) and the left coronary artery (LCA). LCA bifurcates into two arteries – the left circumflex coronary artery (LCX) and the left anterior descending artery (LAD). The calculations were performed for the LCA tree only. Fig. 2 shows a general appearance of the considered LCA tree, and also indicates the locations of the stenosis during simulations. There are several stenoses on one sketch at the same time, but in fact the calculations were carried out several times for each stenosis one by one, i.e., only one stenotic site was present in the LCA branch during each simulation.

The stenosis was introduced into the model as a local narrowing of an artery with a constant radius (i.e., a cylinder), as shown in Fig. 3. The arterial radius was decreased at 3 discretization points, wherein none of them were the point of bifurcation.
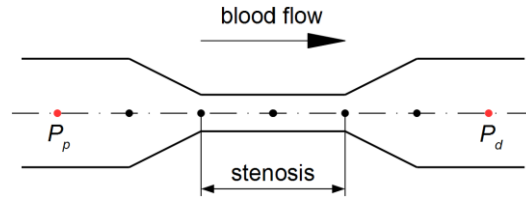
Fig. 3. Schematic model representing the stenosis. Dots show discretization points, red dots indicate points at which proximal pressure (P_p) and distal pressure (P_d) are calculated.

Stenosis is always set in the middle of an arterial branch so there is at least one discretization point without a narrowing between the stenosis and bifurcations. It is important to avoid influence of boundary effects near bifurcations, which can lead to a misestimation of the hydrodynamic resistance caused by the narrowing. Furthermore, our simulations show almost no effect from shifting the stenosis along an arterial branch on the calculated vFFR and VFD.

The stenosis degree (*SD*) was determined by the cross-sectional area, i.e. the cross-sectional area of a stenotic site (A_{st}) was set using the formula:

$$A_{st} = A_n(1 - SD), \tag{4}$$

where A_n is the normal cross-sectional area (i.e. without the stenosis).

The simulations were performed with the stenosis degree values in range 0.20÷0.95.

4   Results

The simulations provided VFD and vFFR values for 9 locations of stenosis with 9 degrees, both for the prescribed inlet flow and for the prescribed pressure. Fig. 4 presents the obtained data.

(A)   (B)
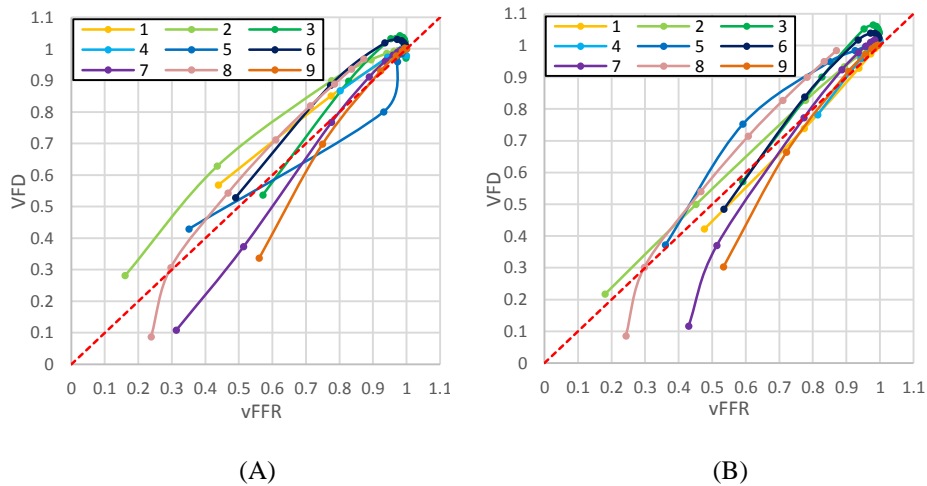
Fig. 4. Plots of relation between VFD and vFFR. The colors correspond to different locations of the stenosis. (A) Prescribed inlet flux scenario; (B) prescribed pressure scenario.

It is clearly seen that, with rare exceptions, the graphs have a similar curved appearance. The points corresponding to lower degrees of the stenosis are located to the right. It can be seen that the greater the stenosis degree, the more points are located below the diagonal. Also, most of the points are to the left of the diagonal line, both for the prescribed inlet flow and for the prescribed pressure, especially in the first case, which indicates that for the specified range of stenosis degree, there are more situations when VFD exceeds vFFR.

The values of vFFR and VFD at approximately the same severe stenosis degree were also considered. Fig. 5 shows the results for the same stenosis locations, but with a stenosis degree equal to 0.85±0.005.
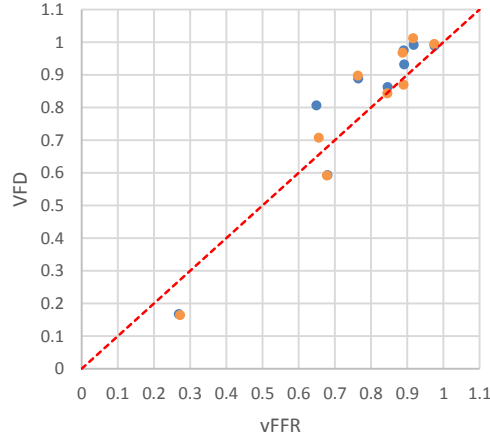
Fig. 5. VFD and vFFR for *SD = 0.85±0.005*. Blue color corresponds to the prescribed inlet flux scenario, orange color corresponds to the prescribed pressure scenario.

The points are located mainly to the left of the diagonal, especially in the high vFFR area (0.8÷1.0). At low vFFR (< 0.4) the points are below the diagonal line. That is, Fig. 5 shows that for a specific degree of stenosis in the range of high vFFR, VFD more often exceeds vFFR, and vice versa for small vFFR. There is also a slight predominance of blue points to the left of the parity line, suggesting that more cases where VFD is greater than vFFR occur in the prescribed flow scenario.

Fig. 4-5 show that in some cases the VFD exceeds 1, which contradicts the equation (2). The possible explanations for this will be given in the next section.

5　Discussion

In this study we have compared virtual FFR-based stenosis assessment to a novel VFD-based assessment, which aims to provide a more accurate measure of stenosis' impact on hemodynamics by directly considering the flux reduction in the stenosed artery.

In the study, nine different stenosis locations were selected. To describe the stenosis location, we consider the number of bifurcations proximal to a stenosis (N_b), the peripherial arterial resistance distal to a stenosis (R_{T0}) and the peripherial arterial resistance of the entire LCA except the branch distal to a stenosis (R_S). The arterial peripheral resistances were calculated only from the terminal resistances, without taking compliance into account, but in the simulations it was also included. Table 2 shows the results obtained by both scenarios for approximately the same $SD = 0.85±0.005$. It can be seen that both scenarios show similar results, and in both cases there are strong differences between the vFFR and VFD for some stenosis locations.

Table 2. Comparison table of the scenarios.

#	A_n, mm^2	N_b	R_{T0}, (N·s)/m^5	R_S, (N·s)/m^5	Prescr. inlet flux		Prescr. pressure	
					vFFR	VFD	vFFR	VFD
1	6.21	1	$1.01 \cdot 10^{10}$	$1.45 \cdot 10^{10}$	0.89	0.93	0.89	0.87
2	3.32	2	$1.17 \cdot 10^{10}$	$1.21 \cdot 10^{10}$	0.65	0.81	0.66	0.71
3	3.08	2	$7.58 \cdot 10^{10}$	$6.47 \cdot 10^{9}$	0.92	0.99	0.92	1.01
4	13.55	1	$1.45 \cdot 10^{10}$	$1.01 \cdot 10^{10}$	0.98	0.99	0.98	0.995
5	2.30	2	$8.77 \cdot 10^{10}$	$6.40 \cdot 10^{9}$	0.77	0.89	0.76	0.90
6	4.81	2	$2.57 \cdot 10^{10}$	$7.76 \cdot 10^{9}$	0.89	0.98	0.89	0.97
7	0.75	3	$2.05 \cdot 10^{11}$	$6.49 \cdot 10^{9}$	0.68	0.59	0.68	0.59
8	0.34	4	$1.18 \cdot 10^{11}$	$6.28 \cdot 10^{9}$	0.27	0.17	0.27	0.17
9	2.67	2	$5.31 \cdot 10^{10}$	$6.72 \cdot 10^{9}$	0.85	0.86	0.85	0.84

For the scenario of prescribed inlet flux, for most cases VFD predicts a lower impact of the stenosis on hemodynamics than vFFR, which agrees with the analytical model presented in Section 2. In particular, for FFR = 0.7, which is associated with severe stenosis [14], there is quite a large spectrum of VFD values, depending on the specific vessel considered. With the exception of sites #5, #9 and #7, the VFD values are larger than vFFR. For FFR = 0.8, which is often recommended as a criterion for intervention [6, 8], the range of VFD values is smaller, and VFD is larger than vFFR for all sites except #5 and #9. This means that FFR-based assessment tends to overestimate the hemodynamic value of the stenosis. This difference between VFD and vFFR persists also for large arteries, for example #1, #4.

The different behavior of #5 in Fig. 4A compared to other plots is not predicted by our analytical estimation. However, the effect disappears in the prescribed pressure scenario that shows that this case is simpler for stenosis assessment. For the prescribed flux case we can only note large number of alternative drains and low total parallel resistance (R_S, see the Table 2) of them, thus the blood flux can be easy distributed among them. Finally, the reason must be a combination of the location of this stenosis and the characteristics of the rest of the blood network in dynamics.

Interestingly, the difference between vFFR and VFD is the largest for intermediate values of vFFR between 0.4 and 0.8, while for very large and very small vFFR this difference is smaller. Also of note is the flow increase for very small stenosis degree values in several cases, so the VFD may be greater than 1. This effect persists for increased equilibration times and reduced timesteps, with the maximal volumetric flow increase of around 3% compared to the no-stenosis case. This may be caused by a numerical effect in the model, or it may be caused by dynamical properties of the flow, somewhat similar to wave impedance in electrodynamics.

For the prescribed pressure scenario, the difference between VFD and FFR is smaller. However, due to the dynamic effects and a more complex geometry than considered for the analytical model, these two measurements are not exactly the same, contrary to the analytical calculation results. VFD is higher than vFFR for the majority of points, except for some severely stenosed cases where it is lower. Similarly to

the prescribed inlet flux case, in two cases there is a minor increase in flow through the stenosis site compared to the baseline. This increase also disappears for larger stenosis degrees.

It is also noticeable that the more distal the stenosis, the stronger the vFFR is correlated with the visual degree of narrowing. It is well-illustrated by Fig. 4.

Overall, this study shows that similar FFR values may correspond to significantly different decreases in pressure, depending on the stenosis location and the ability of the physiology to adapt to the increased resistance. For example, for FFR = 0.8 the model predicts the range of flow decrease from less than 10% to almost 30%. This means that using vFFR as a criterion for stenting may result in performing interventions when they are not really needed. The opposite (not stenting a problematic vessel) is less likely to happen, since we have found few cases where the actual flow was significantly less than what is expected from vFFR (two cases out of the nine considered stenosis positions). Also, vFFR is still a big improvement over a simple visual assessment. A 50% diameter occlusion (a common visual guideline for stenting) can correspond to a very broad spectrum of both vFFR and VFD values.

VFD provides a more direct measure of stenosis impact than vFFR. However, despite that, it would be harder to get VFD-based assessment approved for use in clinical practice than it would be for virtual FFR-based assessment. This is because the quantity of interest provided by VFD is different from the (experimental) FFR used in clinical practice. Hence, to get approval from the regulatory bodies it will be necessary not only to convince them that the VFD values provided by the model are representative of the real artery, but also to demonstrate that VFD is a sensible measure of hemodynamic significance (which is non-trivial, despite VFD being a more direct measurement).

6   Conclusion

The study is devoted to assessment of the physiological importance of a particular arterial stenosis based on CA blood flow simulation. Currently, FFR values are widely used to address this problem. FFR can be either measured invasively or calculated from numerical simulations (vFFR). The latter way currently receives great attention of the modeling community.

However, the FFR does not provide a direct estimation of volumetric flow rate drop caused by a stenosis, which would be the most precise assessment of its physiological impact. Therefore, we have introduced a different parameter called Volumetric Flow Drop (VFD) which is calculated as the ratio of the flux through the stenosis to the flux through the same artery without a stenosis. It shows how the flux through the artery will increase after stenting of the stenosis.

These days many studies that use numerical simulations of blood flow for assessment of the stenosis impact in real clinical practices are being published. Thus, we would like to note that our study is of a different type and we are not presenting any novel methodology of blood flow modeling application. Our goal is to check the relation between FFR and VFD for various positions of stenosis and to detect the cases

when the difference can be considerable. We are not considering a personalized blood flow model and thus all the related issues are out of the scope of this study.

We have shown that FFR and VFD parameters match for a simplified model of CA and only in the case when inlet pressure is prescribed. If the inlet flux is prescribed instead, the FFR value overestimates the VFD. The detailed investigation based on a 1D numerical blood flow model of CA shows that a real relation of FFR and VFD can be even more complex due to omitted complex structure of CA and the pulsatile nature of blood flow. In particular, for FFR = 0.7, which is associated with severe stenosis [13], there is a deviation of VFD values in range of ±0.1 and more, that can have a direct influence on the treatment strategy.

We also would like to note that for the same model of stenosis and the same degree of stenosis a very wide variation of FFR and VFD has been found. This fact also emphasize that the physiological importance of a stenosis is rather related to the global flow pattern in the CA than to the local hydrodynamic resistance of the construction. Accurate calculation of vFFR requires modeling a considerable part of CA just as VFD does; that is confirmed by many related studies of vFFR calculation [8, 9].

For calculating the VFD, the 1D numerical model was used, verified using an analytical model. For the validation clinical data is needed, which is hard to obtain. Therefore, there is a field for further research on the importance of VFD.

Finally, we would like to conclude that the VFD may provide a more accurate estimation of the stenosis physiological importance and can be considerably different from the FFR value. The FFR was introduced as a method of invasive stenosis assessment and presents a compromise between accuracy and ease of *in vivo* measurement. VFD obviously cannot be measured *in vivo* directly, but there are no such limitations for simulation-based virtual measurements. Thus, the approach can be used if there is patient data sufficient to build a computational model. For the purpose of simulation results interpretation VFD provides a more accurate assessment of stenosis importance compared to vFFR.

7   Acknowledgements

References

1. Pijls, N.H.J., de Bruyne, B., Peels, K., van der Voort, P.H., Bonnier, H.J.R.M., Bartunek, J., Koolen, J.J.: Measurement of fractional flow reserve to assess the functional severity of coronary-artery stenoses. N Engl J Med 334, 1703–1708 (1996).
2. Saha, S., Purushotham, T., Prakash, K.A.: Numerical and experimental investigations of fractional flow reserve (FFR) in a stenosed coronary artery. E3S Web of Conferences 128, 02006 (2019).

3. Lotfi, A., Jeremias, A., Fearon, W.F., Feldman, M.D., Mehran, R., Messenger, J.C., Grines, C.L., Dean, L.S., Kern, M.J., Klein, L.W.: Expert consensus statement on the use of fractional flow reserve, intravascular ultrasound, and optical coherence tomography: A consensus statement of the society of cardiovascular angiography and interventions. Catheterization and Cardiovascular Interventions 83, 509–518 (2014).

4. Pijls, N.H.J, van Son, J.A.M., Kirkeeide, R.L., De Bruyne, B., Gould, K.L.: Experimental basis of determining maximum coronary, myocardial, and collateral blood flow by pressure measurements for assessing functional stenosis severit before and after percutaneous transluminal coronary angioplasty. Circulation 87 (4), 1354–1367 (1993).

5. Mehra, A., Mohan, B.: Value of FFR in clinical practice. Indian Heart Journal 67, 77–80 (2015).

6. Briceno, N., Lumley, M., Perera D.: Fractional flow reserve: conundrums, controversies and challenges. Interventional Cardiology 7(6), 543–552 (2015).

7. Morris, P.D., van de Vosse, F.N., Lawford, P.V., Hose, D.R., Gunn, J.P.: "Virtual" (computed) fractional flow reserve: current challenges and limitations. JACC Cardiovasc Interv. 8(8), 1009–1017 (2015).

8. Carson, J.M., Pant, S., Roobottom, C., Alcock, R., Blanco, P.J., Bulant, C.A., Vassilevski, Y., Simakov, S., Gamilov, T., Pryamonosov, R., Liang, F., Ge, X., Liu, Y, Nithiarasu, P.: Non-invasive coronary CT angiography-derived fractional flow reserve: A benchmark study comparing the diagnostic performance of four different computational methodologies. Int J Numer Meth Biomed Engng. 35, e3235 (2019).

9. Crystal, G.J., Klein, L.W.: Fractional flow reserve: physiological basis, advantages and limitations, and potential gender differences. Current Cardiology Reviews 11, 209–219 (2015).

10. Fearon, W.F., Achenbach, S., Engstrom, T., Assali, A., Shlofmitz, R., Jeremias, A., Fournier, S., Kirtane, A.J., Kornowski, R., Greenberg, G., Jubeh, R., Kolansky, D.M., McAndrew, T., Dressler, O., Maehara, A., Matsumura, M., Leon, M.B., De Bruyne, B.: Accuracy of fractional flow reserve derived from coronary angiography. Circulation 139(4), 477–484 (2019).

11. Levy, P.S., Kim, S.J., Eckel, P.K., Chavez, R., Ismail, E.F., Gould, S.A., Ramez Salem, M., Crystal, G.J.: Limit to cardiac compensation during acute isovolemic hemodilution: influence of coronary stenosis. American Journal of Physiology-Heart and Circulatory Physiology, 265(1), H340–H349 (1993).

12. Boileau, E., Nithiarasu, P., Blanco, P.J., Müller, L.O., Fossan, F.E., Hellevik, L.R., Donders, W.P., Huberts, W., Willemet, M., Alastruey, J.: A benchmark study of numerical schemes for one-dimensional arterial blood flow modeling. Int. J. Numer. Meth. Biomed. Engng., 31(10), e02732 (2015).

13. Alastruey, J., Khir, A.W., Segers, P., Sherwin, S.J., Verdonck, P.R., Parker, K.H., Peiró, J.: Pulse wave propagation in a model human arterial network: Assessment of 1-D viscoelastic simulations against in vitro measurements. J Biomech., 44(12), 2250–2258 (2011).

14. Fahmi, R., Eck, B.L., Fares, A., Levi, J., Wu, H., Vembar, M., Dhanantwari, A., Bezerra, H.G., Wilson, D.L.: Dynamic myocardial perfusion in a porcine balloon-induced ischemia model using a prototype spectral detector CT. In: Proc. SPIE 9417, Medical Imaging 2015: Biomedical Applications in Molecular, Structural, and Functional Imaging, 94170Y (2015).